Magnetic control of squeezing effects

1998 J. Phys. A: Math. Gen. 31 309

(http://iopscience.iop.org/0305-4470/31/1/027)

J. Phys. A: Math. Gen. **31** (1998) 309–320. Printed in the UK PII: S0305-4470(98)84761-6

Magnetic control of squeezing effects

Francisco Delgado C† and Bogdan Mielnik‡
Depto de Física, CINVESTAV, AP 14-740, 07000, México DF, México

Received 2 June 1997, in final form 11 September 1997

Abstract. A class of magnetic control operations permitting one to achieve the Brown and Carson effect (shrinking or expansion of the wavepacket in coordinate space) by applying sinusoidal magnetic pulses is presented, with numerical data. An analogue of the Strutt diagramm for the phenomenon is obtained. We show that the scale operation is achieved as a 'boomerang effect'; its repetitions (when applying periodic magnetic pulses), cannot assure the 'monotonic tracking' of the packet size to zero. This is due to a new 'no go argument' which forbids the generation of the multiple squeezing effects without paying a price in the form of intermediate expansions.

1. Introduction

Current techniques for controlling micro-objects are centred mostly on particle trapping and cooling [1–3]. The next step is the fine manipulation of quantum states, including the details of their wave-like behaviour. The subject has several branches, interrelated with control theory [4]. In quantum mechanics this subject was put forward by Lamb Jr [5] (see also [6–10]); in the area of squeezed states by Yuen [11] (see also [12–14]); in molecular physics by Brumer and Shapiro [15], as well as Clark and Huang *et al* [16, 17]; the feedback techniques (tracking) by Rabitz and co-workers [18–20].

In practical terms, one of the major difficulties in manipulating the wavepackets is the infinite dimension of the quantum mechanical space of states (see, e.g., the recent discussion by Clark [16]). However, in 1976 a method for generating squeezed states in $L^2(\mathbb{R})$ was designed by Yuen [11]. An analogue of the spin echo effect for 'continuous degrees' was found in 1977 [7]. In 1985, the provocative essay 'Atomic memory' [21] of Brewer and Hahn formulated an hypothesis about scenarios permitting one to recover the past states of many particle systems (see also [22]). The significance of quantum manipulation for subtle experimental techniques (like that of non-demolishing measurements [23, 24]) was pointed out independently by several authors; see, for example, Yuen, Lynch and Royer [24–26].

One of the most interesting operations upon wavepackets is scale transformation (amplification or contraction). The first study dedicated to this particular effect in $L^2(\mathbb{R})$ was carried out by Brown and Carson [12] in terms of coherent states. The same problem admits alternative approaches in terms of exponential formulae (see Ma and Rhodes [13], Grübl [27], Bechler [28], Baseia *et al* [14]) or in terms of adiabatic invariants (Lewis, Malkin and Dodonov *et al* [29–31]). While mathematically complete, the resulting schemes are not convenient to provide numerical data, which are still missing even for the most natural experimental arrangements.

† Depto de Matemáticas, ITESM, Campus Estado de México, AP 2, 52926, Atizapán, Edo de Mex., México.
‡ Institute of Theoretical Physics, Warsaw University, ul Hoza 69, 00-681, Warsaw, Poland.

0305-4470/98/010309+12$19.50

Below, we shall add a next section to the 'encyclopedia of manipulations' by designing precise prescriptions for squeezing the Schrödinger wavepacket in two space dimensions. Our tool will be a time-dependent homogeneous magnetic field. We are not interested in all types of squeezing effects, but only in coordinate squeezing (the Brown and Carson effect [12]). To be close to laboratory techniques, we shall focus our attention on sinusoidally pulsating fields and currents. We shall then present an analogue of the Strutt diagram for the intensity parameters which generate the exact scale effect (the shrinking or expansion of the Schrödinger packet).

As it sometimes happens when existence theorems are replaced by operational techniques, some new facts emerge. In this case, they offer an alternative for the interesting idea of 'observable tracking' (see [16–20]). We show that while a sequence of multiple squeezings of the wavepacket is quite an elementary phenomenon, it has the character of a 'boomerang' rather than of a 'tracking' effect. This might suggest some new techniques for control theory.

2. The Schrödinger wavepacket in a homogeneous magnetic field

Our system consists of a charged Schrödinger particle in a homogeneous magnetic field $\boldsymbol{B}(t) = B(t)\boldsymbol{n}$ associated with a cylindrically symmetric electric field, both described by the vector potential

$$\boldsymbol{A}(\boldsymbol{x}, t) = -\tfrac{1}{2}\boldsymbol{x} \times \boldsymbol{B}(t) = -\tfrac{1}{2}B(t)\boldsymbol{x} \times \boldsymbol{n} \tag{2.1}$$

where $\boldsymbol{n}$ is a fixed unit vector defining our z-axis. Fields of this geometry are produced in infinite, cylindrical solenoids, with $B(t) = (4\pi/c)I(t)$, where $I(t)$ is the solenoid current density. The space geometry of our field is trivial; the only non-trivial part is the time-dependent $B(t)$. Note also that the expression (2.1) is exact only if $I(t) =$ constant; otherwise, the solenoid currents produce retarded corrections. Computed by applying the $1/c$ development [32], they are of the order of magnitude $\sim\epsilon^2 B(t)$, where $\epsilon = \pi R/cT$, R is the solenoid radius and T is the magnetic pulse period [33], and they are negligible in almost all laboratory conditions; we shall thus stick to (2.1). The corresponding Hamiltonian for the Schrödinger particle is

$$H(t) = \frac{1}{2m}\left(\boldsymbol{p} - \frac{e}{c}\boldsymbol{A}\right)^2 = \frac{1}{2m}p_z^2 - \frac{eB(t)}{2mc}M_z + \frac{1}{2m}\left[p_x^2 + p_y^2 + \left(\frac{eB(t)}{2c}\right)^2 (x^2 + y^2)\right] \tag{2.2}$$

and generates the evolution operator

$$U(t, 0) = \mathrm{e}^{-\mathrm{i}tp_z^2/2m\hbar}\,\mathrm{e}^{(\mathrm{i}/\hbar)\alpha(t)M_z}W_x(t)W_y(t) \tag{2.3}$$

where the first two terms stand for the free propagation along the solenoid axis z and for the rigid rotation around z by the angle

$$\alpha(t) = \frac{e}{2mc}\int_0^t B(\xi)\,\mathrm{d}\xi.$$

The non-trivial part of (2.3) contains two structurally identical evolution operators $W_x(t)$ and $W_y(t)$ describing two twin oscillators in x, p_x and y, p_y (compare [14]).

Below we assume that $B(t)$ repeats some standard pulse pattern in a sequence of intervals $[0, T], [T, 2T], \ldots, [(n-1)T, nT]$, and we shall study the operators $W_x(T)$ and $W_y(T)$, the 'finite analogues' of the Floquet operators for our process. To deal only with the essential

parameters, we introduce the new time $\tau = t/T$ and new dimensionless canonical variables. The evolution equations for $W_x(t)$ and $W_y(t)$ then take the familiar oscillator form [29–31]

$$\frac{\mathrm{d}W}{\mathrm{d}\tau} = -\mathrm{i}G(\tau)W(\tau) \tag{2.4}$$

$$G(\tau) = \frac{p^2}{2} + \beta(\tau)^2\frac{q^2}{2} \tag{2.5}$$

where the pair q, p means either

$$q = \sqrt{\frac{m}{T\hbar}}q_x \qquad p = \sqrt{\frac{T}{m\hbar}}p_x$$

or

$$q = \sqrt{\frac{m}{T\hbar}}q_y \qquad p = \sqrt{\frac{T}{m\hbar}}p_y.$$

$W(\tau)$ is either $W_x(T\tau)$ or $W_y(T\tau)$, and $\beta(\tau) = eTB(T\tau)/2mc$ comprises all essential physical information.

Our aim is to find the 'manipulation function' $\beta(\tau)$ defined in $[0, 1]$ which would generate at $\tau = 1$ an exact scale transformation of the wavepackets $\psi(x)$ (where x is the real variable in the spectrum of q, and λ is the scale constant):

$$\psi(x) \to \psi_\lambda(x) = \frac{1}{\sqrt{\lambda}}\psi\left(\frac{x}{\lambda}\right) \qquad (0 \neq \lambda \in \mathbb{R}). \tag{2.6}$$

While the existence of solutions is granted by the Brown and Carson theorem [12], the purely technical difficulties blocked the study of the laboratory receipts. We shall show below that the easiest way to obtain the detailed numerical data is by using a matrix representation of the evolution operators [30, 31, 34, 35].

3. Quantum evolution and classical trajectories

The matrix picture stems naturally from the Heisenberg scheme [30, 31, 35]. For the quadratic Hamiltonians of form (2.5), the pair of Heisenberg operators $q(\tau) = W(\tau)^* q W(\tau)$, $p(\tau) = W(\tau)^* p W(\tau)$ depend linearly on the initial pair q, p:

$$\begin{pmatrix} q(\tau) \\ p(\tau) \end{pmatrix} = u(\tau)\begin{pmatrix} q \\ p \end{pmatrix} \tag{3.1}$$

and the Schrödinger evolution equations (2.4) and (2.5) for $W(\tau)$ traduces itself into

$$\frac{\mathrm{d}u(\tau)}{\mathrm{d}\tau} = \Lambda(\tau)u(\tau) \qquad u(0) = \mathbf{1} \tag{3.2}$$

where

$$\Lambda(\tau) = \begin{pmatrix} 0 & 1 \\ -\beta(\tau)^2 & 0 \end{pmatrix}. \tag{3.3}$$

It is essential that the relation (3.1) holds in both classical and quantum cases with exactly the same matrix $u(\tau)$ [8, 10, 30]. The columns of $u(\tau)$ correspond, therefore, to the c-number orbits of the classical oscillator (2.5). As observed by Royer, this gives a very simple key to predicting the effects of squeezing (see particularly figure 2 in [35]). Indeed, since in q, p variables the scale transformation reads $q \to \lambda q$, $p \to (1/\lambda)p$, the idea is

to generate the pair of orbits yielding at $\tau = 1$ the canonical transformation (equivalent to (2.6))

$$u(1) = \begin{pmatrix} \lambda & 0 \\ 0 & 1/\lambda \end{pmatrix}. \tag{3.4}$$

We adopt an even simpler variant of this idea. We fix attention on just one classical orbit, departing from $A_0 = (1, 0)$ (i.e. with $q(0) = 1$, $p(0) = 0$), and we shall use it as our 'indicatrix trajectory'. Its general form can be easily read from the Hamiltonian (2.5).

If the function $\beta(\tau)$ in the Hamiltonians (2.5) is fixed, then at any τ, the phase plane is covered by a unique vector field which determines the direction of the trajectory at every point (q, p). However, if $\beta(\tau)$ is manipulable (i.e. $\beta(\tau)$ stands for a wider class of experimentally admissible external forces), then from every point (q, p) sticks not only one but an entire bunch of vectors (in general, in form of a cone), defining the admissible directions in which the trajectory could be continued (figure 1).

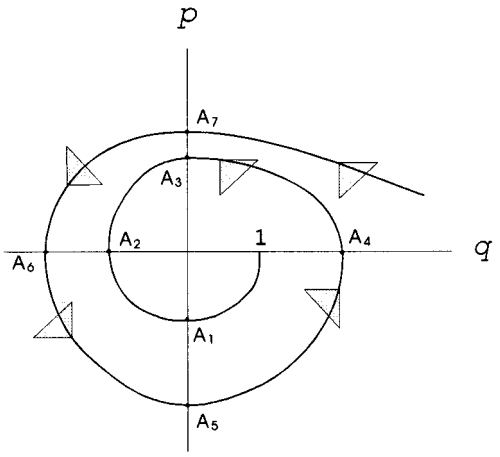

Figure 1. A typical phase trajectory of the classical oscillator (2.5) with a manipulable frequency. The triangles (mobility cones) restrict the admissible tangent vectors of the trajectory. The time moments in which the trajectory intersects the q-axis are the only ones in which the corresponding quantum evolution can produce the scale transformations of the Schrödinger's wavepacket.

The typical phase trajectory of (2.4) and (2.5) must spiral through a sequence of repeating sectors (but if $\beta(\tau)$ vanishes quickly enough as $\tau \to +\infty$, it may escape to $\pm q$-infinity after a finite number of turns). We assume that our 'indicatrix orbit' turns around the centre, intersecting the q-axis one or more times. (Note, that too weak $\beta(\tau)^2$, e.g. $\beta(\tau)^2 < \pi^2$ for all $\tau \in [0, 1]$, cannot ensure this; cf comparison theorems, Hille [36, p 394]. Now let $A_1, A_2, A_3, \ldots$ be the points and $\tau_1, \tau_2, \tau_3, \ldots$ the time moments in which our trajectory intersects the q and p axes. Consider the evolution matrices $u_1, u_2, u_3, \ldots$ generated in the subsequent time intervals $[0, \tau_1], [\tau_1, \tau_2], [\tau_2, \tau_3], \ldots$, i.e. $u_i = u(\tau_i, \tau_{i-1})$. The matrix u_1 brings the initial point $A_0(q = 1, p = 0)$ to $A_1(q = 0, p = -a_1; a_1 > 0)$; hence

$$u_1 = \begin{pmatrix} 0 & 1/a_1 \\ -a_1 & b_1 \end{pmatrix}. \tag{3.5}$$

In turn, u_2 transforms $A_1(q = 0, p = -a_1)$ into $A_2(q < 0, p = 0)$; and so, it must be of the form

$$u_2 = \begin{pmatrix} b_2 & 1/a_2 \\ -a_2 & 0 \end{pmatrix}. \tag{3.6}$$

Thus, the evolution matrix associated with the wider time interval $[0, \tau_2] = [0, \tau_1) \cup [\tau_1, \tau_2]$ is

$$u(\tau_2, 0) = u_2 u_1 = \begin{pmatrix} -a_1/a_2 & (a_1 b_1 + a_2 b_2)/a_1 a_2 \\ 0 & -a_2/a_1 \end{pmatrix}. \tag{3.7}$$

Now if the pair (b_1, b_2) is orthogonal to (a_1, a_2), the matrix (3.7) becomes diagonal, yielding a scale transformation with a negative scale constant $\lambda = -a_1/a_2$. Notice that the subsequent evolution matrices corresponding to the next intersections of our trajectory with q and p axes repeat the general forms of (3.5) and (3.6), although the coefficients may differ. Consistently, the points $A_1, A_3, A_5, \ldots$ are the only ones in which the evolution operator can (though needs not) become a generalized Fourier transformation ($q \to -\zeta p$, $p \to \zeta^{-1} q$), whereas the points $A_2, A_4, A_6, \ldots$ are the only ones where it may become a scale transformation (with the scale constant negative for $A_2, A_6, \ldots$ and positive for $A_4, A_8, \ldots$).

We shall look for solutions when the evolution operator becomes the scale transformation for some $\tau = \tau_{2n} = 1$ (choosen to be our time unit). Our method will consist of integrating (analytically or numerically) the classical motion trajectories for (3.2) and selecting the cases when the matrix (3.7) accepts the form (3.4).

4. Exact solutions

Up until now, the only exact solution to (3.4) has been obtained by Grübl [27], for $B(t)$ being a step function with two constant values $B_1 \neq B_2$ in two subintervals $[0, T_1), [T_1, T] \subseteq [0, T]$. In the reduced variables

$$\beta(\tau) = \begin{cases} \alpha_1 & \text{for } 0 \leqslant \tau < \tau_1 \\ \alpha_2 & \text{for } \tau_1 \leqslant \tau \leqslant 1 \end{cases} \tag{4.1}$$

where $\alpha_i = eTB_i/2mc$ $(i = 1, 2)$, $\tau_i = T_i/T$. The simplest proof that β-jumps (4.1) can generate scale transformations is obtained in terms of the evolution matrix $u(1)$ which becomes the product of two matrices induced by constant magnetic fields in $[0, \tau_1)$ and $[\tau_1, 1]$:

$$u(1) = \begin{pmatrix} \cos(\alpha_2\tau_2) & \sin(\alpha_2\tau_2)/\alpha_2 \\ -\alpha_2 \sin(\alpha_2\tau_2) & \cos(\alpha_2\tau_2) \end{pmatrix} \begin{pmatrix} \cos(\alpha_1\tau_1) & \sin(\alpha_1\tau_1)/\alpha_1 \\ -\alpha_1 \sin(\alpha_1\tau_1) & \cos(\alpha_1\tau_1) \end{pmatrix}. \tag{4.2}$$

Now, whenever

$$\alpha_1\tau_1 = (n + \tfrac{1}{2})\pi \qquad \alpha_2\tau_2 = (k + \tfrac{1}{2})\pi \tag{4.3}$$

where n, k are two arbitrary integers, both factors of (4.2) acquire the desired form (3.5) and (3.6) (of two generalized Fourier matrices with the diagonal terms $b_1 = b_2 = 0$) and the evolution process in $[0, 1]$ produces a scale transformation:

$$\begin{aligned} u(1) &= \begin{pmatrix} 0 & (-1)^n/\alpha_2 \\ (-1)^{n+1}\alpha_2 & 0 \end{pmatrix} \begin{pmatrix} 0 & (-1)^k/\alpha_1 \\ (-1)^{k+1}\alpha_1 & 0 \end{pmatrix} \\ &= (-1)^{n+k+1} \begin{pmatrix} \alpha_1/\alpha_2 & 0 \\ 0 & \alpha_2/\alpha_1 \end{pmatrix}. \end{aligned} \tag{4.4}$$

The evolution operator $U(T)$ given by (2.3), apart of the transformation (4.4) in x, p_x and y, p_y, generates a rotation on the xy plane; however, if (4.3) holds, the rotation contributes just to another $(-1)^{n+k+1}$, and $U(T)$ generates the pure scale transformation†

$$\begin{aligned} U(T)^* x U(T) &= \lambda x \qquad & U(T)^* p_x U(T) &= \lambda^{-1} p_x \\ U(T)^* y U(T) &= \lambda y \qquad & U(T)^* p_y U(T) &= \lambda^{-1} p_y \end{aligned} \tag{4.5}$$

with

$$\lambda = \alpha_1/\alpha_2. \tag{4.6}$$

The corresponding Schrödinger wavepacket $\psi(x, y, z)$, consistently undergoes a free evolution in the z-direction and the scale transformation on the xy plane. In an infinitely long solenoid, an initial state described by

$$\mathrm{e}^{\mathrm{i}kz}\Psi(x, y) \tag{4.7}$$

after the two-pulse operation (4.1)–(4.3) must become

$$\mathrm{e}^{\mathrm{i}\varphi}\,\mathrm{e}^{-\mathrm{i}(kz-\omega T)}\lambda^{-1}\Psi(\lambda^{-1}x, \lambda^{-1}y) \qquad (\varphi \in \mathbb{R}). \tag{4.8}$$

Note that the packet expansions are obtained for $|a_1| > |a_2|$; (the stronger pulse first, the weaker one later); the contractions, inversely, require $|a_1| < |a_2|$ (the weaker pulse first, the stronger one later). The effect is well illustrated by congruences of classical trajectories propagating in the rectangular pulses (4.1) (see figure 2).

After rectangular pulses (distinguished by their mathematical simplicity), next in importance are sinusoidal pulses (distinguished by their laboratory merits). While the analytic solutions are not known, the effect can be described with any desired accuracy by the trajectory method. For simplicity, we have choosen the magnetic field composed of the static (background) and sinusoidal parts:

$$B(t) = B_0 + B_1 \sin(\omega t - \delta) \Rightarrow \beta(\tau) = \alpha_0 + \alpha_1 \sin(2\pi\tau - \delta) \tag{4.9}$$

where $\alpha_j = eB_jT/2mc$. Our task was to determine the Floquet matrix $u(1)$ for the oscillator process (3.2) induced by the field (4.9). As a 'survey region', we have choosen a rectangle in the three-dimensional space $\mathbb{R}^3$ of the dimensionless parameters $\boldsymbol{a} = (\alpha_0, \alpha_1, \delta)$:

$$\Theta = [-12, 12] \times [-12, 12] \times [0, 2\pi] = \boldsymbol{A} \times [0, 2\pi]. \tag{4.10}$$

As the basic invariant $\Delta = \mathrm{Tr}\,u(1)$ does not depend on the phase δ, the Floquet theory for equations (3.2) and (3.3) permits the prediction (see Reed and Simon [37]) that $\boldsymbol{A} = [-12, 12] \times [-12, 12]$ must be a sum of two domains: $\boldsymbol{A}_\mathrm{s}$ in which $|\Delta| < 2$ and the iterations of $u(1)$ can produce only the limited orbits (the stability region); $\boldsymbol{A}_\mathrm{i}$, in which $|\Delta| \geqslant 2$ and the iterations $u(1)^n = u(n)$, $(n = \ldots, -1, 0, 1, \ldots)$ yield diverging trajectories (the instability region). The divisory line $\partial\boldsymbol{A}_\mathrm{s}$ is an analogue of the *Strutt diagramm* known in the theory of Mathieu functions. To obtain more details, the domain Θ was covered by a net of 10^6 points in which the numerical integration of (3.2) and (3.3) was carried out, giving $u(1)$ for every point of the net. The computer was then asked to interpolate, finding: (1) the set $\boldsymbol{S} \subset \boldsymbol{A}_\mathrm{i}$ of pairs (α_0, α_1) ('scale points') for which the scale transformation can be achieved at $\tau = 1$ for some $\delta \in [0, 2\pi]$, (2) for any $(\alpha_0, \alpha_1) \in \boldsymbol{S}$ the values of δ, for which the scale transformation indeed occurs and (3) the corresponding values of the scale constant λ. We found that $\boldsymbol{S}$ forms a curve ('scale diagramm', see figure 3), defining the first structure detail on the otherwise black chart of the instability area.

† The matrix demonstration (4.2)–(4.8) is relatively recent [33]. Grübl himself, had no confidence to the operator formulae; he found (4.8) working with the Gaussian wavepackets [27].

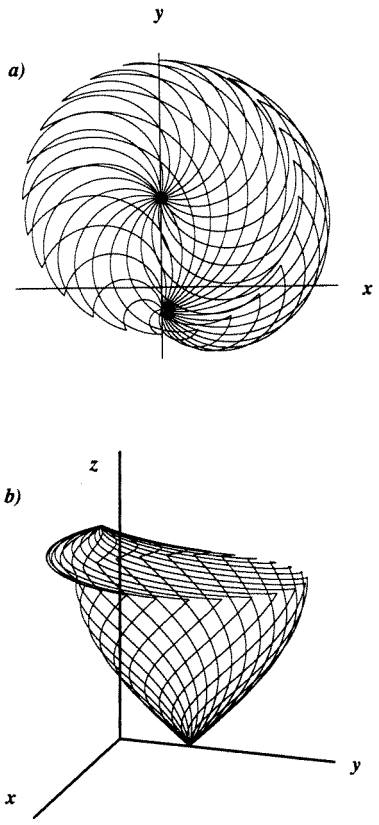

Figure 2. The magnetic Grübl mechanism. (a), (b) two views of a congruence of classical trajectories in presence of a squeezing two-pulse pattern (2.1)–(2.5) with $\beta(t)$ of the form (4.1)–(4.3) for $|\lambda| < 1$. The trajectories diverge from a common initial point with a common initial v_z to focus again, λ times closer to the z-axis ($\lambda \simeq \frac{1}{3}$).

Observe that since our 'manipulation function' $\beta(\tau) = eB(T\tau)T/2mc$ is dimensionless, all mathematical results are translated unambiguously (independently of the units) into physical conditions. Thus, for α_0, α_1 in the white area (e.g. for $|\alpha_0| + |\alpha_1| < \pi$) there is no squeezing—which might mean that B_0, B_1 are too small, but also that the particle is too heavy or that the operation time T is too short. The best scale effects (in our search region) are achieved for the sequence of 'dark points' presented in table 1.

To check the results we have fed the magnetic intensities and the phase from the top row of table 1 into the Lorentz equation and examined congruences of classical trajectories. Figure 4 shows a congruence, diverging from a single point at $\tau = 0$ with a common initial velocity component v_z, to be focused at $\tau = 1$ in a new point, closer to the solenoid axis.

By examining the trajectories, we have noticed a curious effect (apparently overlooked in the traditional theory of squeezing). The squeezing is never achieved as a *monotonic shrinking* of a congruence of trajectories, but has a nature of a 'boomerang effect': in order to focus, the trajectories must first dramatically diverge; the focusing then comes as an 'end surprise' (figure 5). The persistence of this mechanism, visible for both Grübl and sinusoidal cases indicates some general law behind.

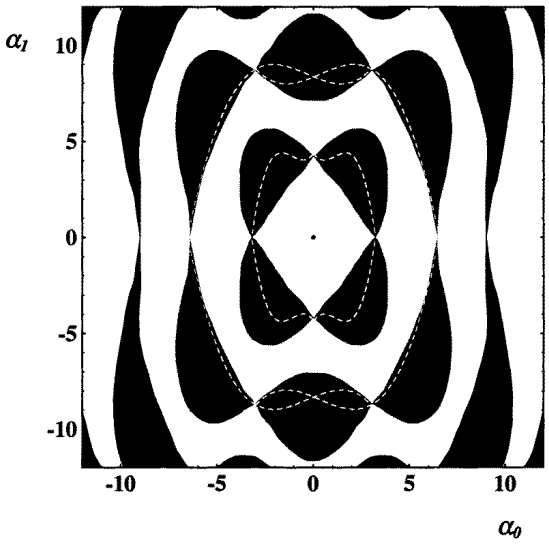

Figure 3. The first structure detail on the instability chart (black) for the sinusoidal magnetic pulses. The interrupted white line ($\boldsymbol{S}$) collects the points (field amplitudes) (α_0, α_1) for which the Floquet operator becomes the exact scale transformations for some $\delta \in [0, 2\pi]$.

Table 1. Numerical data about the sinusoidal pulses generating the best scale effects: the selected points (magnetic intensities) on the scale curve of figure 3; the corresponding phases granting the scale transformations; the amplification constants.

$(\alpha_0, \alpha_1) \in \boldsymbol{S}$	δ	λ
(−1.000 00, 9.775 39)	0.950 00	4.108 43
	2.190 31	0.244 50
	4.007 81	4.108 43
	5.416 10	0.244 50
(0.699 90, 8.765 76)	1.020 97	4.139 94
	2.119 98	0.241 50
	4.251 75	4.139 94
	5.172 33	0.241 50
(2.299 00, 3.580 10)	0.662 08	−3.327 13
	2.479 46	−0.300 66
(2.55555, 3.13286)	0.637 26	−3.225 15
	2.504 27	−0.310 10

5. The mechanism of counter-effects

In fact, there exists a simple proof of the inseparability of contractions and expansions for one-dimensional oscillators (2.5). This inseparability turns out a general law independent of the particular shape of the oscillator pulses.

Proposition. (*Counter-effect lemma*). Let $\beta(\tau)$ in (2.5) be any bounded, periodic function of period 1. Suppose that the evolution defined by the Hamiltonian (2.5) produces a scale transformation for $\tau = 1$ (and its iterations for $\tau = n = 1, 2, 3, \ldots$). Then there exists a

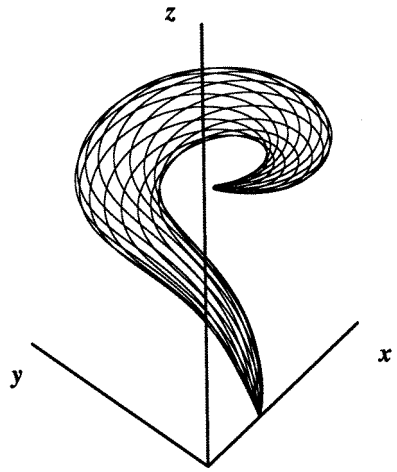

Figure 4. A shrinking congruence generated by sinusoidal magnetic pulses for the triple of parameters of figure 3, $s_3 = (2.2990, 3.5801)$, $\delta_3 = 2.416\,25$. The congruence diverges from a common point with a common initial v_z to produce a new focus, 0.3008 times closer from the solenoid axis z.

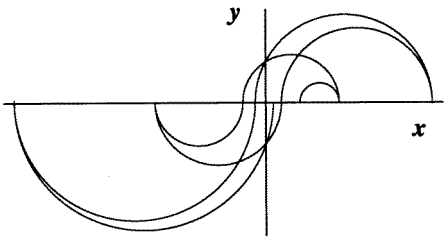

Figure 5. A trajectory in the form of arcs generated by a repeated Grübl pattern with $|\lambda| < 1$. Notice a curious boomerang effect: the closer the trajectory approaches to the centre at the end of every two-pulse period, the further away it must slip in the intermediate time moments (compare with section 5).

sequence of intermediate time moments $\tau = \tau_1 + n$ $(n = 0, 1, 2, \ldots)$ such that the same process produces the inverse scale transformation in any time interval $[\tau_1 + n, \tau_1 + n + 1]$.

Proof. Assume that the matrix $u(\tau)$ takes the form (3.4) for $\tau = 1$. The indicatrix trajectory departing from $(q = 1,\ p = 0)$ at $\tau = 0$ thus arrives at $(q = \lambda,\ p = 0)$ at $\tau = 1$. Before this happens, it must intersect (at least once) the negative p axis (figure 1). Suppose, this happens at some $\tau = \tau_1$ $(0 < \tau_1 < 1)$, at a point $q(\tau_1)$ $(q = 0,\ p = -a_1 < 0)$. This means that the matrix $u_1 = u(0, \tau_1)$ must be of the form (3.5) and $u_2 = u(\tau_1, \tau_2)$ of the form (3.6) (see the discussion in section 3). Since we assume that the product of both matrices $u_2u_1 = u(1)$ is a (diagonal) scale transformation (3.4), hence $a_1b_1 + a_2b_2 = 0$. If the fields are periodic and the pattern repeats, the entire evolution process is driven by an infinite sequence of matrices; $u_1, u_2, u_1, u_2, u_1, \ldots$. In particular, for any $\tau = n$, the evolution matrix is

$$u(n) = u_2u_1u_2u_1 \ldots u_2u_1 = (u_2u_1)^n \tag{5.1}$$

whereas at $\tau = \tau_1 + n$

$$u(\tau_1 + n) = (u_1 u_2)^n u_1. \tag{5.2}$$

Notice now that if $a_1 b_1 + a_2 b_2 = 0$ and

$$u_1 u_2 = \begin{pmatrix} b_1 & 1/a_1 \\ -a_1 & 0 \end{pmatrix} \begin{pmatrix} b_2 & 1/a_2 \\ -a_2 & 0 \end{pmatrix} = \begin{pmatrix} \lambda & 0 \\ 0 & 1/\lambda \end{pmatrix} \tag{5.3}$$

then simultaneously

$$u_1 u_2 = \begin{pmatrix} 0 & 1/a_2 \\ -a_2 & b_2 \end{pmatrix} \begin{pmatrix} b_1 & 1/a_1 \\ -a_1 & 0 \end{pmatrix} = \begin{pmatrix} 1/\lambda & 0 \\ 0 & \lambda \end{pmatrix}. \tag{5.4}$$

Henceforth, an inavoidable side effect of a sequence of the scale transformations (3.4) in the intervals $[n, n+1]$ is the sequence of the inverse scale transformations in $[\tau_1 + n, \tau_1 + n + 1]$, $n = 0, 1, 2, \ldots$. □

In physical terms our lemma permits us to interpret the 'boomerang effect' as the typical manipulation of the *heating area* carried out under conditions of energy resonance between the particle and the field pulses. The mechanism can be used to achieve an (instantaneous) cooling, when the packet is amplified, momenta reduced, energy emitted to the external field. However, if the periodic pulses are not interrupted, the opposite occurs: the packet shrinks, the energy is re-absorbed and momenta are amplified.

A practical consequence is the limit which the size of the solenoid imposes not only on the expansions, but also upon the contraction effects. A more general conclusion is evidently the importance of non-perturbative effects as an alternative branch of the control technology.

6. Practical and fundamental aspects

The field magnitudes and some limitations of our procedures must be discussed. Since the values of the dimensionless parameters $\alpha\tau = eBT\tau/2mc$ are fixed by (4.3), the required pulse intensities are inversely proportional to the operation time T as well as to the ratio e/m of the micro-object (a property shared by some other manipulation schemes involving magnetic fields [9, 10, 38]). Thus, for example, in order to shrink the wavefront of an electron $\lambda = 10^4$ times, within $T = 10^{-3}$ s, a pair of relatively weak magnetic pulses of $\simeq 10^{-5}$ G and $\simeq 10^{-1}$ G acting for 0.9999×10^{-3} s and 10^{-7} s is sufficient. For the proton, the pulses should be around 2000 times stronger. For a strongly charged 'semimacroscopic particle' with a mass $m = 10^{-15}$ g and charge $q = 1000e = 10^{-7}$ esu the scale contraction with $\lambda = 10^{-3}$ taking $T = 1$ s would involve magnetic pulses of very high intensity $\simeq 10^6$ G. However, if the object travels slowly along the solenoid axis, the experimentalist may have time enough to accomplish a longer (or iterated) operation with weaker fields (the orders of magnitude are similar for Grübl and sinusoidal cases). Although the shrinking effect lasts only an instant, some additional methods might help to perpetuate it. Quite conveniently, the shrinking operation *starts* with a weaker pulse and *ends up* with a stronger one: this makes it possible to keep the beam narrow by simply mantaining the strong magnetic field after the end of the operation.

It seems that this scheme might work as an alternative mechanism to focus particle beams. The operations of the expansion (amplification [12]), $|\lambda| > 1$, open up even more temptating perspectives. First, it would be interesting to exploit technically the diffractionless, amplified images (4.8). To scan the 'instantaneous pictures' involves the

problems of time control. Note, however, that the very techniques of time selection have been successfully applied elsewhere (see, e.g., the 'coincidence optics' reported in [39]).

Some fundamental aspects of the 'amplification operation' are no less attractive. According to orthodox quantum mechanics the macroscopic objects, in principle, should possess the same wave-like properties as microparticles. Neutron spectroscopy seems to confirm this idea for nucleon packets extended over a space of several centimetres [40–42]. Recent experiments with sodium and beryllium atoms expand the limits still further [43–45]. Yet, the validity of the superposition principle for heavier bodies is the subject of continuing discussion (see Legget [46], Caldeira and Legget [47], Greenberger [48], Poyatos *et al* [49]; an opposite view in Diosi [50], Ghirardi *et al* [51]; see also the gravitational hypothesis by Penrose [52]). The main difficulty in bringing the discussion into the experimental arena is the absence of techniques to create 'macroscopic superposition' [46]. For 'huge micro-objects' the de Broglie waves [53] diffract slowly and the wavepackets propagate in the form of 'needle beams', with very narrow wavefronts [54]. An idea occurs to us that, for charged particles, one remedy might be the two-dimensional scale transformation (4.5)–(4.8), a process which can pump the wavefront to any desired size without affecting the coherence. If so, the magnetic operation (4.5) and (4.6) ($\lambda > 1$) might be a correct method to call into existence the '*macroscopic superposition*', if it exists at all.

Acknowledgments

The authors are grateful to their colleagues in the Department of Physics of CINVESTAV, Mexico, for their interest in this work and helpful discussions. Thanks are due to Constantin Piron, Jean Pierre Eckmann, Charles Enz and Jan Chroboczek for their interest in the subject and comments on the focusing operation and to Jerzy Kowalczynski and Riccardo Capovilla for pertinent comments on the macroscopic superpositions. The support of CONACYT is acknowledged.

References

[1] Brown L S and Gabrielse G 1986 *Rev. Mod. Phys.* **58** 233
[2] Stemholm S 1986 *Rev. Mod. Phys.* **58** 699
[3] Phillips W D and Metcalf H J 1987 *Sci. Am.* **256** 36
[4] See, e.g., the monographs: Wiener N 1961 *Cybernetics or Control and Communication in the Animal and the Machine* (New York: MIT)
Bellman R 1967 *Introduction to the Mathematical Theory of Control Processes* vol 1, 2 (New York: Academic)
[5] Lamb W E Jr 1966 *Phys. Today* **22** 23
[6] Lubkin E 1974 *J. Math. Phys.* **15** 663
Lubkin E 1974 *J. Math. Phys.* **15** 673
[7] Mielnik B 1977 *Rep. Math. Phys.* **12** 331
[8] Mielnik B 1986 *J. Math. Phys.* **27** 2290
Mielnik B 1989 **30** 550 (Erratum)
[9] Fernández C D 1992 *Nuovo Cimento* B **107** 885
[10] Fernández C D J and Mielnik B 1994 *J. Math. Phys.* **35** 2083
[11] Yuen H P 1976 *Phys. Rev.* A **13** 2226
[12] Brown L S and Carson L J 1979 *Phys. Rev.* A **20** 2486
Brown L S 1987 *Phys. Rev.* A **36** 2463
[13] Ma X and Rhodes 1988 *Phys. Rev.* A **39** 1941
[14] Baseia B, Mizrahi S S and Moussa M H Y 1992 *Phys. Rev.* A **46** 5885
[15] Brummer P and Shapiro M 1994 *Sci. Am.* **272** 34
Brummer P and Shapiro M 1992 *Anu. Rev. Phys. Chem.* **43** 257 and the literature therein
[16] Clark J 1996 *Condensed Matter Theories* vol 11 (Commack, NY: Nova Science)

[17] Huang G M, Tarn T J and Clark J W 1983 *J. Math. Phys.* **24** 2608
Tarn T J, Clark J W and Huang G M 1989 *Modeling and Control of Systems* ed A Blaquiere (Berlin: Springer)
[18] Chen Y, Gross P, Ramakrishna V and Rabitz H 1995 *J. Chem. Phys.* **102** 8001
[19] Gross P, Singh H, Rabitz H, Mease K and Huang G M 1993 *Phys. Rev.* A **47** 4593
[20] Gross P, Ramakrishna V, Villalonga E, Rabitz H, Littman M, Lyon S and Shayegan M 1994 *Phys. Rev.* B **49** 100
[21] Brewer R G and Hahn E L 1984 *Sci. Am.* **251** 50
[22] Waniewski J 1980 *Commun. Math. Phys.* **76** 27
[23] Caves C M, Thorne K S, Drewer R W P, Sandberg V D and Zimmermann M 1980 *Rev. Mod. Phys.* **52** 341
[24] Yuen H P 1983 *Phys. Rev. Lett.* **51** 719
[25] Lynch R 1984 *Phys. Rev. Lett.* **52** 1729
[26] Royer A 1987 *Phys. Rev.* A **36** 2460
[27] Grübl G 1988 *J. Phys. A: Math. Gen.* **37** 2985
[28] Bechler A 1988 *Phys. Lett.* **130A** 481
[29] Lewis H R 1968 *J. Math. Phys.* **9** 1976
Lewis H R and Riesenfeld W B 1969 *J. Math. Phys.* **10** 1458
[30] Malkin A, Man'ko V I and Trifonow D A 1973 *J. Math. Phys.* **14** 576
[31] Dodonov V V, Malkin I A and Man'ko V I 1975 *J. Phys. A: Math. Gen.* **8** 19
Dodonov V V, Malkin I A and Man'ko V I 1975 *Int. J. Th. Phys.* **14** 37
[32] Infeld L and Plebanski J 1960 *Motion and Relativity* (Warsaw: PWN and Pergamon)
[33] Delgado C F 1992 Manipulación electromagnética del paquete de Onda *Master Thesis* CINVESTAV, México
[34] Wolf K B 1974 *J. Math. Phys.* **15** 1295
[35] Royer A 1993 Understanding squeezing of quantum states with a Wigner function *Proc. III IWSSUR* ed D Han *et al* (NASA Conf. Publ. 3322) p 269
[36] Hille E 1969 *Lectures on Ordinary Differential Equations* (Reading, MA: Addison-Wesley)
[37] Reed M and Simon B 1978 *Methods of Modern Mathematical Physics, IV, Analysis of Operators* (New York: Academic)
[38] Mielnik B and Fernández C D J 1989 *J. Math. Phys.* **30** 537
Fernández C D J and Mielnik B 1990 *Phys. Rev.* A **41** 5789
[39] Shih G, Sergienko A, Pittman T T, Strekalov D and Klyshko D 1995 Two-photon 'ghost' image and interference-diffraction *Proc. IV ICSSUR* ed D Han *et al* (NASA Conf. Publ. 3322) p 169
[40] Badurek G, Rauch H and Tuppinger D 1986 *Phys. Rev.* A **34** 2600
[41] Rauch H 1988 *Microphysical Reality and Quantum Formalism* ed A J van der Merwe *et al* (Dordrecht: Kluwer) p 161
[42] Summhammer J, Rauch H and Tuppinger D 1987 *Phys. Rev.* A **36** 4447
[43] Schmiedmayer J, Chapman M, Ekstrom C, Hammond T, Wehinger S and Pritchard D 1995 *Phys. Rev. Lett.* **74** 1043
[44] Chapman M, Ekstrom C, Hammond T, Schmiedmayer J, Wehinger S and Pritchard D 1995 *Phys. Rev. Lett.* **74** 4783
[45] Kwiat P, Weinfurter H and Zeilinger A 1996 *Sci. Am.* Nov., 52
[46] Leggett A J 1984 *Contemp. Phys.* **25** 583
[47] Caldeira O and Leggett A J 1983 *Ann. Phys.* **149** 374
[48] Greenberger D M 1983 *Rev. Mod. Phys.* **55** 875
[49] Poyatos J F, Cirac J I and Zoller P 1996 *Phys. Rev. Lett.* **77** 4728
[50] Diosi L 1989 *Phys. Rev.* A **40** 1165
[51] Ghirardi G, Rimini A and Weber T 1986 *Phys. Rev.* D **34** 470
Ghirardi G, Grassi R and Pearle P 1990 *Found. Phys.* **20** 1271
Ghirardi G, Grassi R and Pearle P 1992 *Phys. Lett.* **166A** 435
[52] Penrose R 1995 Quantum theory and reality *Shadows of the Mind* (Oxford: Oxford University Press) ch 6
[53] de Broglie L 1925 *Ann. Phys.* **2** 22
[54] Bagrov V G, Belov V V and Ternov I M 1983 *J. Math. Phys.* **24** 2855